JSEE Vol. 21, No. 3, 2019 DOI:10.48303/jsee.2019.241709

Research Note

Detection of Long-Range Correlations and Trends Between Earthquakes in California

Yasaman Maleki[1] and Mostafa AllamehZadeh[2]*

1. Assistant Professor of Statistics, Faculty of Mathematical Sciences, Alzahra University, Tehran, Iran
2. Assistant Professor of Earthquake Engineering, IIEES, Tehran, Iran,
* Corresponding Author; email: mallam@iiees.ac.ir

Received: 15/12/2018
Accepted: 09/02/2020

ABSTRACT

In this paper, we investigate the long-range correlations and trends between consecutive earthquakes by means of the scaling parameter so-called locally Hurst parameter, H(t), and examine its variations in time, to find a specific pattern that exists between Earthquakes. The long-range correlations are usaully detected by calculating a constant Hurst parameter. However, the multi-fractal structure of earthquakes caused that more than one scaling exponent is needed to account for the scaling properties of such processes. Thus, in this paper, we consider the time-dependent Hurst exponent to realize scale variations in trend and correlations between consecutive seismic activities, for all times. We apply the Hilbert-Huang transform to estimate H(t) for the time series extracted from seismic activities occurred in California during 12 years, from 2/24/2007 to 9/29/2017. The superiority of the method is discovering some specific hidden patterns that exist between consecutive earthquakes, by studying the trend and variations of H(t). Estimationg H(t) only as a measure of dependency, may lead to misleading results, but using this method, the trend and variations of the parameter is studying to discover hidden dependencies between consecutive earthquakes. Recognizing such dependency patterns can help us in prediction of future main shocks.

Keywords:
Long-range dependence; Time-dependent Hurst exponent; Hilbert-Huang transform; Empirical mode decomposition; Seismic activities

1. Introduction

Earthquakes are complex phenomena to analyze. Seismic data as time series exhibit complex patterns, as they encode features of the events that have occurred over extended periods of time, as well as information on the disordered morphology of rock and its deformation during the time that the events were occurring. It is for such reasons that seismic records appear seemingly chaotic. Numerous papers have reported that large events are preceded by anomalous trends of seismic activity both in time and space. Several reports also indicate that seismic activity increases as an inverse power of the time to the main event (sometimes referred to as an inverse Omori law for relatively short time spans), while others document a quiescence, or even contest the existence of such anomalies at all. If such anomalies can be analyzed and understood, then one might be able to forecast future large events.

One of the most interesting properties that time series of different kinds of phenomena exhibit, is the long-range correlation, also known as long memory or long-range persistence, means that the auto-covariance function decays exponentially, by a spectral density that tends to infinity [1]. Self-similar processes have been used successfully to model data exhibiting long memory and arising in a wide variety of fields, ranging from physics

(geophysics, turbulence, hydrology, solid-state physics, ...) or biology (DNA sequences, heat rate variability, auditory nerves spike trains, ...), to human operated systems (telecommunications network traffic, image processing, pattern recognition, finance, ...) [2].

For self-similar (or scale invariant) processes, the probabilistic properties of the process remain invariant when it is viewed at different time-scales. In mathematical expression, a stochastic process $\{X(t),\ t \in R^+\}$ is scale invariant or self-similar with Hurst parameter *H*, if for all $\lambda > 0$ it follows the scaling law: $X(\lambda t) \equiv \lambda^H X(t),\ t \in R^+$, where $\equiv$ means equality in all finite dimensional distributions [3]. The index *H* characterizes the self-similar behavior of the process, and a very large variety of methods has been proposed in the literature for estimating it [4-6].

Earthquakes are an example of complex phenomena that are scale invariant and fractal in their collective properties. These properties are revealed both in nature and laboratory experiments where the spatial, temporal and size distributions of earthquakes or laboratory acoustic emissions display structures that are invariant in scale [7-9]. The emergence of these properties is indicative of complexity and nonlinear dynamics in the earthquake generation process, such that concepts like fractals and multifractals are becoming increasingly fundamental for understanding geophysical processes and estimating seismic hazard more efficiently. Therefore, time series of earthquakes are widely used to characterize the main features of seismicity and to provide useful insights into the dynamics of the seismogenic system. The complex phenomenology exhibited by earthquakes is due to the deformation and sudden rupture of parts of the earth's crust because of the external forces acting from plate tectonic motions [10].

Detecting the long-range power-law correlations between consecutive earthquakes is regarded as a main feature in studying seismic activities. This property traditionally measured by the scaling Hurst parameter, which allows distinguishing the persistence (correlation), anti-persistence (anti-correlation) or randomness of the data [11]. Until now, the Hurst exponent is estimated as a constant parameter for the whole seismic data process. However, based on the multi-fractal structure of seismic data, considering only one Hurst exponent for the whole process, may lead to misleading results. Therefore, to study the short or long-range dependence in seismic activities, more than one scaling exponent is needed to account for the scaling properties of such processes, which reflects the occurrence of different dynamics at different time-scales, and the local variations of roughness can be described by allowing the Hurst exponent to vary with time [12]. References [6, 13-16] studied this family of self-similar processes, and estimated the local Hurst parameter $H(t)$.

In spite of wide application of approaches based on nonlinear dynamics methods, the Fourier and wavelet transformations, etc., there are essential limitations, which narrow down the range of applicability of the results obtained. One of the main difficulties is that seismic data are discrete signals, which is not taken into account. Another factor, which should be taken into account is the influence of local time effects. Alongside the discreteness and the local behavior of the seismic signals, is the influence of long-range memory effects.

Now, in this work, to detect the long-range correlations that exist between foreshocks, main shock and the aftershocks corresponds to earthquakes that occurred during 12 years in California (Figure 1), we estimate the Hurst exponent locally using the empirical mode decomposition (EMD) and the Hilbert-Huang transform (HHT). The Hurst exponent, that also called *H* index of long-range dependence, is a measure of long-term memory of a time series. It quantifies the tendency of a time series either to regress to the mean value, or to cluster in a direction. The Hurst exponent was introduced in the analysis of hydrological data by [17]. By applying this method, at first, the time series of earthquakes decomposes into several oscillatory modes by means of empirical mode decomposition, and then, the Hilbert transform is applied to these oscillations to obtain time varying attributes. The time-dependent scaling properties of seismic data are associated with the relative weights of the amplitudes at characteristic frequencies.

The main contribution of the paper is investigating the trend and time-dependent autocorrelation

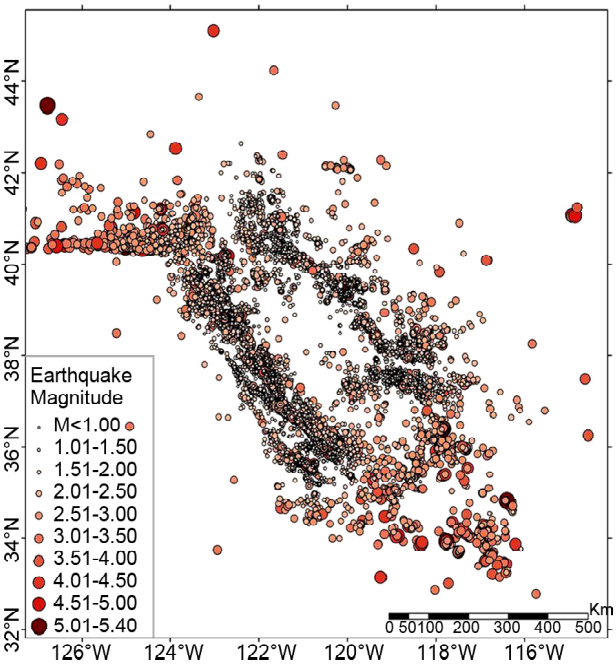

Figure 1. The map shows the earthquakes occurred in California during 24 February 2007 to 29 September 2017.

patterns that exist between consecutive seismic activities occurred around great earthquakes. This study will help us to find a specific hidden pattern that exists between seismic activities that leads to main shocks and prediction of them. For this end, we should study some earthquakes in a special area, that in this paper we consider earthquakes in California during 10 years and define the main shocks as earthquakes with magnitudes greater than 6. Then, its foreshocks and aftershocks are considered as earthquakes occurred three days before and seven days after the main shock, respectively. Thus, we construct some intervals in the time index, which consist of foreshocks, main shock and the aftershocks correspond to those earthquakes, and then calculate the exponent for all times in the intervals. By this method, the Hurst exponent is estimated locally and so, we can detect short and long memory behavior exist between consecutive seismic activities. However, we should notify that, in spite of the importance of estimating $H(t)$, we should know that considering only the value of this parameter may lead to misleading results. Because, most of the time, we estimate $H(t)$ for seismic data as a measure less than or equal to 0.5, which shows a stochastic behavior of seismic activities. But, in fact, there is a great dependancy among earthquakes that are not shown by only computing the value of $H(t)$. Thus, in addition of estimating the locally Hurst parameter, we should study its trends and variations in time to discover some hidden patterns which declare us great earthquakes. Therefore, we propose a new method in discovering such hidden trends by studying the behavior of $H(t)$ in time. Thus, we can detect some trends that exist among foreshocks and their relationships to occuring the main shock, and also between the main shock and its aftershocks. Using this method, some hidden patterns exist among consecutive earthquakes are realized, where at first glance, it seems that they are happening randomly, but in fact they are strongly dependent. As an example, we have studied earthquakes happened during 10 years in California that contain six main shocks to show this kind of hidden trends and correlations that repeated regularly in all six great earthquakes.

The paper is organized as follows: In Section 2, we review the Hilbert-Huang transform and the methodology used for estimation of $H(t)$. In Section 3, the performance of the method is evaluated for simulated data, and then we apply the method to estimate the time-dependent Hurst exponent for investigating the long-range correlations and trends between foreshocks, main shock and the aftershocks of seismic activities occurred in California during 10 years, from 2/24/2007 to 9/29/2017.

2. Methodology

To describe nonlinear distorted waves in detail, along with the variations of these signals that occur naturally in nonstationary processes, the HHT was developed. As is well known, the data analysis methods for nonlinear and nonstationary processes provide very limited options. The natural physical processes are mostly nonlinear and nonstationary, where the available methods are either for linear but nonstationary, or nonlinear but stationary and statistically deterministic processes [18]. Thus, the HHT was developed to provide an alternative view of the time-frequency-energy paradigm of data. In this approach, the nonlinearity and nonstationarity can be dealt with better than by using the traditional paradigm of constant frequency and amplitude. One way to express the

nonstationarity is to find instantaneous frequency and instantaneous amplitude. This was the reason why Hilbert spectrum analysis was included as a part of it [19]. The HHT consists of two steps: namely, the empirical mode decomposition and the Hilbert transform. In this section, we will introduce briefly both components of HHT and present some properties of HHT.

The EMD decomposes the time series into a set of intrinsic mode functions (IMFs), and the Hilbert transformation of these IMFs provides local frequency and amplitude attributes [20]. The EMD is a fully adoptive decomposition that does not require any a priori basis systems. The purpose of the method is to identify oscillating components of the process with scales defined by the local maxima and the minima of the data itself. Hence, given a time series $Y(t)$, $t = 1, 2, \ldots, N$, the EMD decomposes it into a finite number of IMFs denoted as $\delta_k(t)$, $k = 1, \cdots, n$ and a residue function, $\varepsilon(t)$. The IMFs are components oscillating around zero and obtained through a sifting process, which uses the local extrema to separate oscillations starting with the highest frequency. At the end of the sifting process, the time series $Y(t)$ can be expressed as:

$$Y(t) = \sum_{k=1}^{n} \delta_k(t) + \varepsilon(t) \tag{1}$$

where the residue function, $\varepsilon(t)$, is the non-oscillating drift of the data [21].

First, the EMD method pre-processes the time series and then the Hilbert transform is applied. The easiest way to compute the instantaneous frequency is by using the Hilbert transform, through which the complex conjugate $\hat{\delta}_k(t)$ of any real valued function $\delta_k(t)$ can be determined by:

$$\hat{\delta}_k(t) = \mathcal{H}[\delta_k(t)] := \frac{1}{\pi} \int_{-\infty}^{\infty} \frac{\delta_k(\tau)}{t - \tau} d\tau \tag{2}$$

where the integral has a singular point at $\tau = t$ and it is defined as a Cauchy principal value [22]. In this case, a complex function $\tilde{Z}_k$, would be defined as $\tilde{Z}_k(t) = \delta_k(t) + \hat{\delta}_k(t) = a_k(t) e^{i\phi_k(t)}$, with amplitude $a_k(t)$ and phase $\phi_k(t)$ that are defined as follows:

$$a_k(t) = \sqrt{\delta_k^2(t) + \hat{\delta}_k^{\,2}(t)}, \quad \phi_k(t) = \tan^{-1} \frac{\hat{\delta}_k(t)}{\delta_k(t)} \tag{3}$$

Also, the instantaneous frequency is defined as the derivative of the phase, $\phi_k(t)$, with respect to the time:

$$\omega_k(t) = \frac{\phi_k(t)}{dt} \tag{4}$$

The time-dependent Hurst estimation method proposed in [20], was constructed by observing how the local amplitudes $a_k(t)$ in Equation (3), change with respect to the local periods $\tau_k(t) = \omega_k^{-1}(t)$ for all $k = 1, 2, \cdots, n$. The estimation method was first applied to the fractional Brownian motion (fBm), and empirically observed that the amplitude function obtained through the HHT follows a power-law behaviour with respect to the instantaneous period as:

$$a_k(t) \propto \tau_k^{H(t)}(t) \tag{5}$$

where the time-dependent Hurst exponent describes the local scaling properties of the IMF amplitudes and takes values distributed around the Hurst parameter of fBm [20].

3. Simulations Results

To investigate the accuracy of the method in Hurst estimation and so in detection of long-range dependence, first we apply the method for simulated data, and then we estimate the Hurst parameter locally for California seismic activities. To this end, first, we have generated a fBM with scale exponent H=0.6 and length 10000. Then, the HHT method is applied and the $H(t)$ is estimated for all $t \in [1, 10000]$. Figure (2) shows the simulated fBm. Also, the estimated time-dependent Hurst exponent for the simulated fBm is depicted in Figure (3) for all times t = 1 to 10000. The mean and standard deviation of the estimated $H(t)$, are computed as 0.5957697 and 0.0079905, respectively. Evidently, the mean is very close to the Hurst exponent 0.6 with very small variance, which shows the accuracy of the estimation method.

For inquiring the accuracy of the estimation method, we have simulated m = 100 sample paths of fBm with length T=10000 and different Hurst parameters H = 0.1, 0.2, ..., 0.9. Then, the time-dependent Hurst exponent, $H(t)$, is estimated for each time. The time-dependent sample mean for each t is calculated as $\overline{H(t)} = \frac{1}{m} \sum_{j=1}^{m} H_j(t)$. Also, we

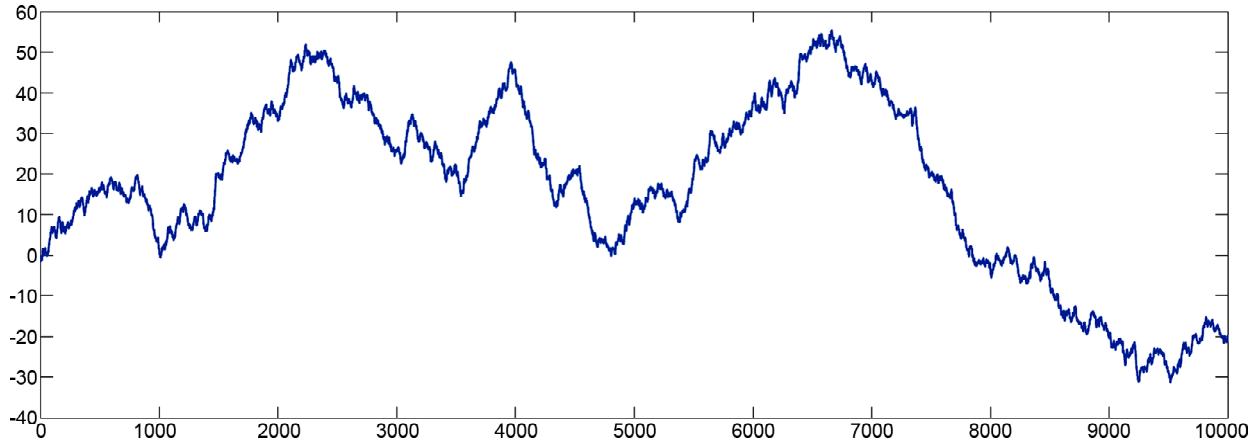

Figure 2. A simulated fractional Brownian motion with length T=10000 and Hurst exponent H=0.6.

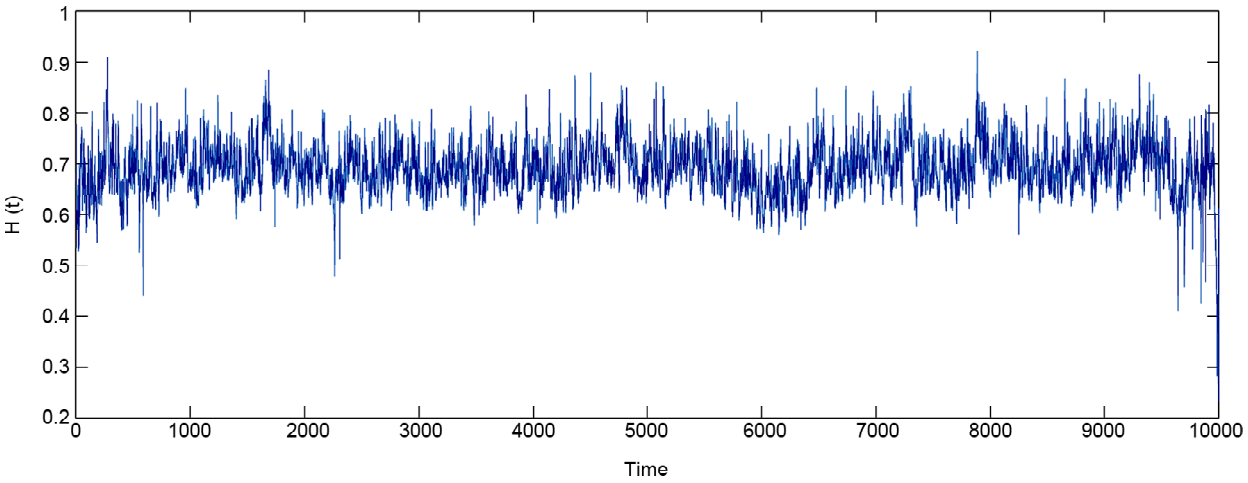

Figure 3. The estimated time-dependent Hurst exponent for the simulated fBm in Figure (2), for all times in t = 1 to 10000.

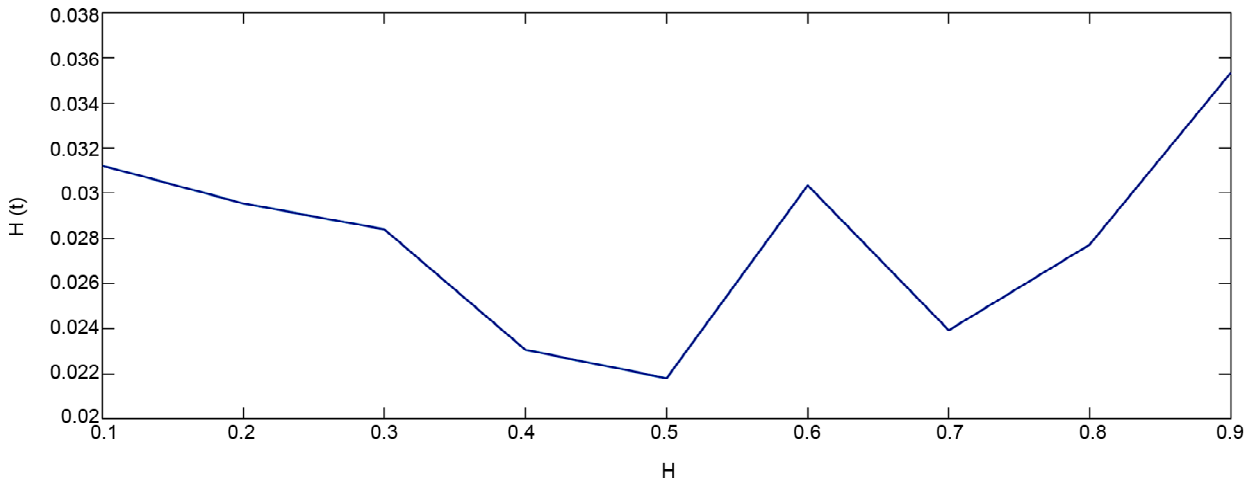

Figure 4. Mean-square of errors of time-dependent Hurst parameter estimation in 100 repetition of fBm for H = 0.1, ..., 0.9.

calculated the mean square of errors (MSE) of the estimation as $MSE = \frac{1}{mT}\sum_{j=1}^{m}\sum_{t=1}^{T}\left(H_j(t) - H\right)^2$, where H is the Hurst parameter of a fBm that we have simulated, and $H_j(t)$ is the Hurst exponent estimated from the *j-th* sample path simulated from fBm. Figure (4) shows the MSEs of $H(t)$ for different Hurst parameters $H = 0.1, ..., 0.9$.

4. Local Hurst Analysis of Seismic Data

Now, in this section, we apply the HHT method for empirical data. In this case, we investigate whether

there exist a long-memory pattern between the consecutive seismic data, by measuring the Hurst exponent locally. Also, we can check how the main shocks are related to the foreshocks and the aftershocks. To study the long-memory behavior between foreshocks, main shock and the after shocks precisely, we consider earthquakes in California during 10 years, beginning with the earthquake occurred on 2/24/2007 and ending with the earthquake on 9/29/2017. As noted before, most of the time, dealing with real world data, the Hurst parameter is not constant for the whole process that may change in time. Therefore, to investigate accurately the long-range correlations between consecutive earthquakes, the time-dependent Hurst exponent should be computed. However, computing $H(t)$ for the whole process, which consists of earthquakes occurred during 10 years would be confusing and can not lead to an accurate and acceptable result. In order to enhance the applicability of the estimation method in detection of long-range dependence between earthquakes, we consider some subintervals of the process, where the parameter $H(t)$ is estimated locally for consecutive earthquakes of each subinterval, separately. First, we choose only great earthquakes, which in this paper we consider only the ones with magnitudes greater than 6. Then, each subinterval is constructed based on the main shock, and its fore and aftershocks, where we consider three days before and seven days after the main shocks as periods for foreshocks and after shocks, respectively. Then, the time-dependent Hurst parameter is estimated for all times in each subinterval. This procedure in selecting subintervals, enabling us to characterize explicitly the correlations exist between the fore and aftershocks, and also discovering hidden dependencies and trends exist between consecutive earthquakes. Figure (5) shows the 38895 seismic activities with magnitudes greater than 1.1 occurred in California from 2/24/2007 to 9/29/2017.

In this study, we have considered seismic activities in a special area for 10 years to distinguish a long-memory pattern that exists between foreshocks, main shock and the aftershocks, based on the locally Hurst parameter. Studying the behavior of $H(t)$, enables us to model how the consecutive earthquakes are correlated, and its variations in time helps us to distinguish hidden trends and also the relationship between foreshocks that leads to the main shock. To this end, we have considered earthquakes with magnitudes greater than 6 as a main shock, and seismic activities for three days before and seven days after the main shock as foreshocks and aftershocks, respectively. As we have seen below, there exists a precise pattern between so many earthquakes, which at first glance, it seems that they were happened randomly, but in fact they are strongly dependent. One reason for considering 10 years earthquakes is to show this kind of correlation pattern in so many earthquakes, which may be used as a precise tool in predicting main shocks [23-26].

4.1. LRD Detection Between Fore and Aftershocks

At first, we consider the first great earthquake

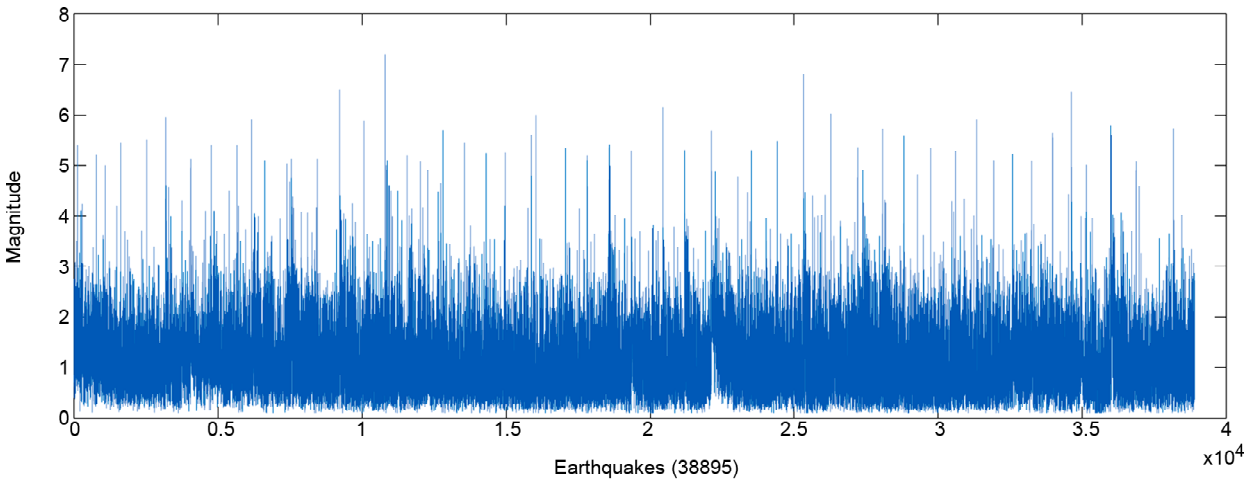

Figure 5. Time-series of magnitudes for seismic activities occurred in California during 24 February 2007 to 29 September 2017, (38895) earthquakes.

that happened in the subinterval of time, consisting of seismic activities occurred on 8th to 17th January 2010. Then, we study the behavior of the estimated time-dependent Hurst parameter to discover hidden trends and correlatons between consecutive earthquakes, which leads to the main shock, and after that the dependencies goes to zero. Figure (6) (top) shows the estimated time-dependent Hurst exponent, where this parameter is less than 0.5 for all times. Therefore, by considering the values of $H(t)$, we may conclude that all earthquakes occurred randomly. However, by considering the times that earthquakes happened and comparing the values of $H(t)$ against the corresponding magnitudes in Figure (7) (top), it should be noted that the values of $H(t)$ are increasing in time, and the autocorrelation between foreshocks, and also foreshocks and the main shock, which occurred on 1/10/2010, enhanced.

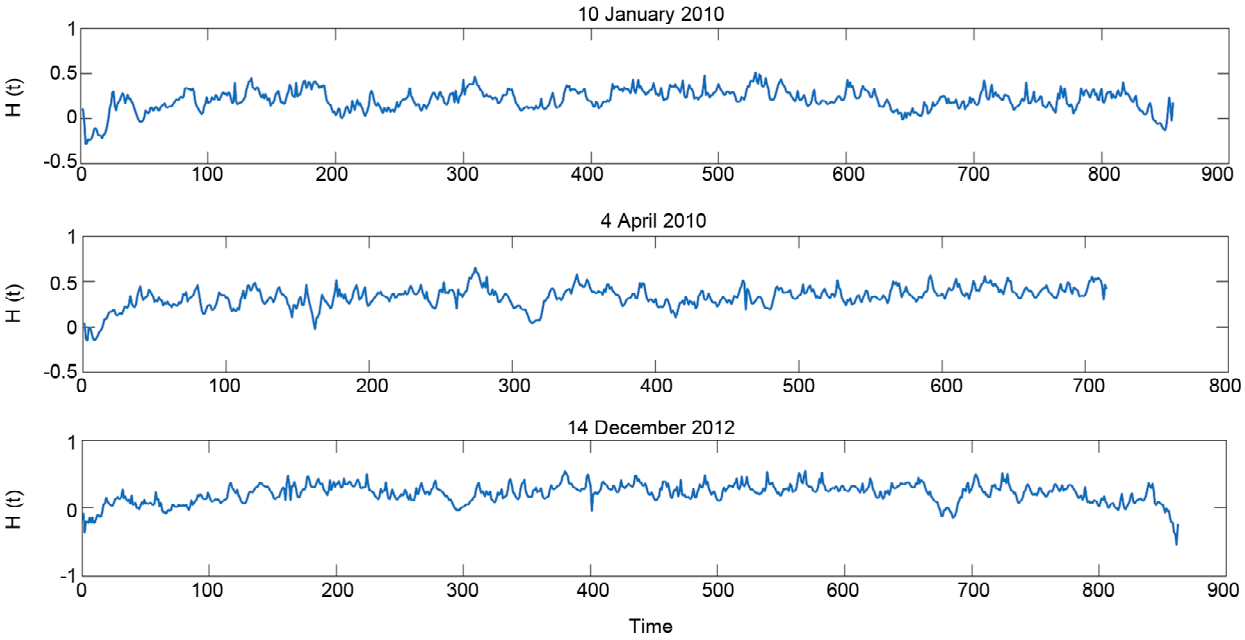

Figure 6. The estimated time-dependent Hurst exponent, H(t), for seismic activities occurred in California, where the time intervals consist of three days before and seven days after the main shock, that the main shocks occurred in: January 2010 (top), April 2010 (middle), and December 2012 (bottom).

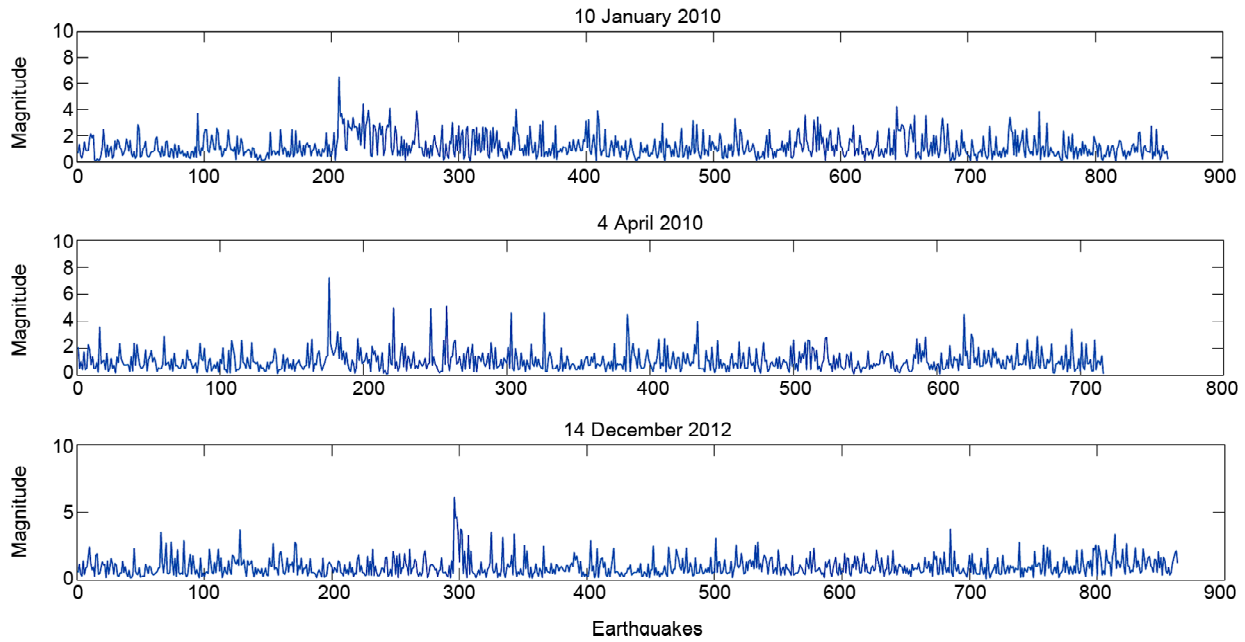

Figure 7. The magnitudes time series for seismic activities occurred in California, where the time intervals consist of three days before and seven days after the main shock, that the main shocks occurred in: January 2010 (top), April 2010 (middle), and December 2012 (bottom).

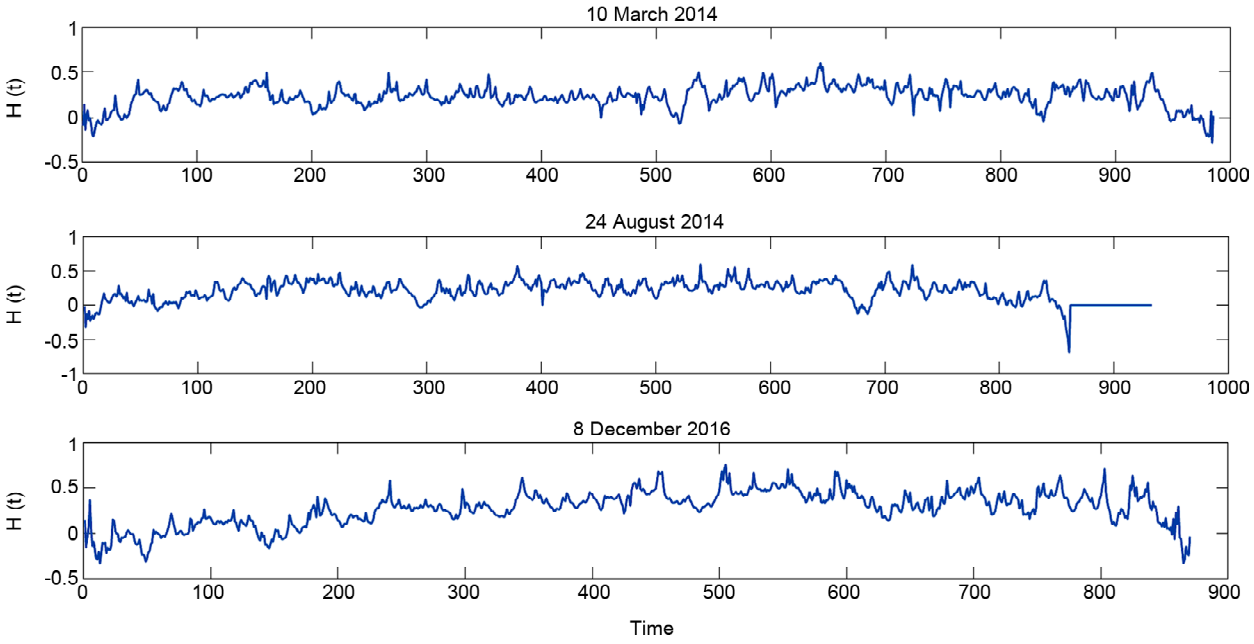

Figure 8. The estimated time-dependent Hurst exponent, H(t), for seismic activities occurred in California, where the time intervals consist of three days before and seven days after the main shock, that the main shocks occurred in: March 2014 (top), August 2014 (middle), and December 2016 (bottom).

After the main shock happened, the Hurst parameter still grows till 1/13/2010, which shows that the autocorrelation between aftershocks are increasing. As it can be seen in Figure (7) (top), there is only one peak in the plot which corresponds to earthquakes that happened on July 13, 2010. By comparing Figures (6) and (8) (top), we realize that six earthquakes with magnitudes near 4 happened until 1/12/2010 that caused such an increasing trend in $H(t)$. In this case, in spite of the values of $H(t)$ that shows the random behavior, by this technique we detect a strong relationship between foreshocks where increased till the main shock happened, and also there are strong dependencies between aftershocks that goes to zero after some big earthquakes.

Next, we consider earthquakes that happened on 2nd to 11th April 2010. The time-dependent Hurst parameter is estimated for all times and the plot is depicted in Figure (6) (middle). As it can be seen in this plot, which shows the behavior of $H(t)$ in time, we realize that the Hurst parameter for foreshocks are less than 0.5, and so we may conclude that they were happening randomly. However, the parameter $H(t)$ was increasing till the main shock occurred on 4/4/2010. Then, the Hurst parameter is still increasing until it reaches to $H(t) = 0.65$, which corresponds to aftershocks until 5/4/2010, and after that the autocorrelation between aftershocks decreases. By comparison of this Figure with its Magnitude counterparts in Figure (7) (middle), we realize that three aftershocks with magnitudes 5, 4.9 and 5.1 happened on 5/4/2010, and the first peak corresponds to their aftershocks (aftershocks of these three earthquakes). Other peaks in the figure also show the great autocorrelation between aftershocks especially for 10th and 11th October 2010, about one week after the main shock, and after that the autocorrelation between aftershocks decreases evidently.

Figure (6) (bottom) shows the behavior of $H(t)$ in time, for seismic activities occurred on 12th to 21st December 2012. In this plot, we also see that the values of $H(t)$ for all foreshocks are less than 0.5, and so the autocorrelations between consecutive earthquakes are weak. Just considering the values of H(t), may lead to the result that the foreshocks were happening randomly. However by considering the trend in the values of $H(t)$, and also by comparing the values of $H(t)$ versus time and magnitudes that they were happened (Figure 7 (top)), we realize that the values of $H(t)$ are increasing in time till 12/13/2010, and then the parameter $H(t)$ decreases until the main shock with magnitude 6.14, happened on 12/14/2010. It should be notified that when the Hurst exponent decreases on 13th

December, the time-series of magnitudes is also decreasing (Figure 6 (bottom)), which shows that there is no dependence between activities, and so they were happening randomly. On the other hand, when we do not expect an earthquake, the main shock with magnitude 6.14 happened. After the main shock, the Hurst parameter is increasing in time till 20th December (six days after the main shock), which is shown as a peak in Figure (7) (bottom). After that the Hurst parameter shows a random behavior in aftershocks, which means the aftershocks were happenning randomly.

Now, we study the autocorrelation between consecutive earthquakes happened during 8th to 17th March 2014. The values of $H(t)$ are depicted in Figure (8) (top). In this plot, we also see that the values of the Hurst parameter for foreshocks are less than 0.5 which may provide a misleading result that the foreshocks occurred randomly. However regarding the increasing trend in $H(t)$ leads to the result that the autocorrelation between consecutive earthquakes raised until they reached to 0.5 that correspond to foreshocks happened on 3/9/2014. Then, the autocorrelation between foreshocks decreased to $H(t) = 0.04$, and when the autocorrelation is near zero, the main shock happened with magnitude 6.8 on 3/10/2014, Figure (9) (top). After the main shock, the Hurst parameter increased again for aftershocks happened on 10th March, where we have two aftershocks with magnitude greater than 4.35. During three days after the main shock, there is not a significant trend in $H(t)$ values. But the autocorrelation between aftershocks decreased to a value near 0, on 3/10/2014, and then an earthquake occurred with magnitude 4.41. We should notify that, the same as before, when the value of $H(t)$ goes to zero and we do not expect an earthquake, it happens. Again, as we have seen in this plot that the autocorrelation between consecutive aftershocks increased and we have significant autocorrelation between aftershocks on 14th March. For the rest of aftershocks, the Hurst parameter varies between 0 and 0.45, and then it vanishes.

The behavior of the estimated parameter $H(t)$ for seismic activities during 22nd to 31st August 2014 are depicted in Figure (8) (middle). Based on values of the time-dependent Hurst exponent, we conclude that the foreshocks were happening randomly and there is not any significant dependence between foreshocks and the main shock, which occurred on 8/24/2014 with magnitude 6.02. In spite of the fact that the foreshocks happened randomly, the figure shows that the Hurst parameter were increasing till the main shock occurred, and after that the estimated $H(t)$ for aftershocks increased only for the day that the main shock happened and then the Hurst parameter decreased. Moreover, there are some peaks in the figure that illustrates the significant autocorrelation between the aftershocks. By comparison with Figure (9) (middle), it can be seen that the peaks in Figure (8) (middle) corresponds to aftershocks of earthquakes that happened with magnitude greater than 3. It should be noted that, we first consider a subinterval that consists of earthquakes occurred during 22nd to 31st August 2014, in which there is not any significant long-range dependence behavior in fore and aftershocks. But if we consider seismic activities in aftershocks with magnitude greater than 3, some long-range dependence specified between their aftershocks.

For earthquakes occurred during 6th to 15th December 2016, as it can be seen in Figure (8) (bottom), there are short-range dependence between foreshocks and also between foreshocks and the main shock, which occurred on 12/09/2016. After the main shock, the autocorrelations between aftershocks are increasing and some peaks are evidently seen in the figure, where the time-dependent Hurst parameter is estimated greater than 0.5, which shows that there is a long-range dependence between aftershocks for about seven days, and after that the autocorrelation decreases and aftershocks randomly occurred.

5. Conclusions

We investigate the autocorrelations exist between foreshocks, main shock and the aftershocks in seismic activities occurred in California during 10 years, from 2/24/2007 to 9/29/2017. We can measure this autocorrelation by means of the Hurst parameter. However, dealing with real-world data, considering a constant parameter for the whole process may lead to misleading results. Therefore, we consider time-dependent Hurst parameter, which can vary with time. Using such a time-dependent

parameter, we are able to estimate the autocorrelation between consecutive earthquakes. However, most of the time, considering only the value of $H(t)$ may lead to misleading results. In this paper, we have shown such situations where the Hurst parameter shows the random behavior in occurring earthquakes, but there are strong correlations between foreshocks that lead to main shock. We have shown this strategy in predicting main shocks by checking the $H(t)$ pattern in time, for six great earthquakes that happenned during 10 years in California, and we have realized that this pattern is repeated for all earthquakes. Thus, we conclude that, considering only the value of $H(t)$ may lead to misleading results and can not help us in predicting main earthquakes. However, we notify that we should check carefully the pattern of the parameter, to detect hidden strong correlations between consecutive earthquakes. To inquire how the Hurst parameter varies in time in foreshocks and aftershocks, we select some subintervals of time in the whole process, in which each subinterval consists of a main shock with magnitude greater than 6 and its fore and aftershocks. Then, we estimate the Hurst parameter for all times in subintervals by means of the Hilbert-Huang transform and empirical mode decomposition method.

References

1. Martin-Montoya, L.A., Aranda-Camachob, N.M., and Quimbayc, C.J. (2014) Long-range correlations and trends in Colombian seismic time series. *Physica A: Statistical Mechanics and its Applications*, **421**, 124-133.
2. Flandrin, P. and Abry, P. (1999) Wavelets for scaling processes. Fractals, *Springer*, 47-64, London.
3. Borgnat, P., Amblard, P.O., and Flandrin, P. (2005) Scale invariances and lamperti transformations for stochastic processes. *J. Phys. A.*, **38**(10), 2081-2101.
4. Bardet, J.M., Lang, G., Oppenheim, G., Philippe, A., Stoev, S., and Taqqu, M.S. (2003) Semiparametric estimation of the long-range dependence parameter: a survey. Theory and applications of long-range dependence. *Birkhuser Boston, Boston,* MA.
5. Beran, J. (1994) *Statistics for Long-Memory Processes*. Monographs on Statistics and Applied Probability. Chapman and Hall, New York.
6. Coeurjolly, J.F. (2001) Estimating the parameters of a fractional Brownian motion by discrete variations of its sample paths. Stat. *Inference Stoch. Process*, **4**(2), 199-227.
7. Main, I. (1996) Statistical physics, seismogenesis, and seismic hazard. *Rev. Geophys.*, **34**(4), 433-462.
8. Sammonds, P.R., Meredith, P.G., and Main, I.G. (1992) Role of pore fluids in the generation of seismic precursors to shear fracture. *Nature*, 359, 228-230.
9. Turcotte, D.L. (1997) *Fractals and Chaos in Geology and Geophysics*. Cambridge University Press, Cambridge, UK, 2nd Ed.
10. Michas, G., Vallianatos, F., and Sammonds, P. (2013) Non-extensivity and long-range correlations in the earthquake activity at the West Corinth rift (Greece), Nonlin, *Processes Geophys.*, **20**, 713-724.
11. Mandelbrot, B.B. and Wallis, J.R. (1968) Noah, Joseph and the operational hydrology. *Water Resour. Res.*, **4**(5), 909-918.
12. Cajueiro, D.O. and Tabak, B.M. (2004) The Hurst exponent over time: testing the assertion that emerging markets are becoming more efficient. *Physica A: Stat. Mech. Appl.*, **336**(3-4), 521-537.
13. Cavanaugh, J.E., Wang, Y., and Davis, J.W. (2003) *Locally Self-Similar Processes and Their Wavelet Analysis. Stochastic Processes: Modelling and Simulation, Handbook of Statist.* North-Holland, Amsterdam.
14. Goncalves, P. and Abry, P. (1997) Multiple-window wavelet transform and local scaling exponent estimation. *IEEE Int. Conf. on Acoust. Speech and Sig. Proc.*, Munich, Germany.
15. Kent, J.T. and Wood, A.T.A. (1997) Estimating the fractal dimension of a locally self-similar Gaussian process by using increments. *J. Roy. Statist. Soc. Ser. B*, **59**(3), 679-699.

16. Stoev, S., Taqqu, M.S., Park, C., Michailidis, G., and Marron, J.S. (2006) LASS: a tool for the local analysis of self-similarity. *Comput. Statist. Data Anal.*, **50**(9), 2447-2471.

17. Hurst, H.E. (1951) Long-term storage capacity of reservoirs. *Transactions of the American Society of Civil Engineers*, **116**, 770-808.

18. Huang, N. E. (2014) Introduction to the Hilbert Huang Transform and Its Related Mathematical Problems, Hilbert-Huang Transform and Its Applications, World Scientific.

19. Carmona, R., Hwang, W.L., and Torresani, B. (1998) P*ractical Time-Frequency Analysis: Gabor and Wavelet Transform with an Implementation in S, Academic*. San Diego, California.

20. Noemi, N., Tiziana, D.M., and Tomaso, A. (2016) Time-dependent scaling patterns in high frequency financial data. *Eur. Phys. J. Special Topics*, **225**, 1997-2016.

21. Huang, N.E., Shen, Z., Long, S.R., Wu, M.C., Shih, H.H., Zheng, Q., Yen, N.C., Tung, C.C., and Liu, H.H. (1998) The empirical mode decomposition and the Hilbert spectrum for nonlinear and non-stationary time series analysis. *Proc. R. Soc. London, A*, **454**(1971), 903-998.

22. King, F. (1997) *Encyclopedia of Mathematics and its Applications*. Cambridge University Press, Cambridge.

23. Farrokhi, M., Hamzehloo, H., Rahimi, H., and AllamehZadeh, M. (2016) Separation of intrinsic and scattering attenuation in the crust of central and eastern Alborz region. *Physics of the Earth and Planetary Interiors*, **253**, 88-96.

24. Farrokhi, M., Hamzehloo, H., Rahimi, H., and AllamehZadeh, M. (2015) Estimation of coda-wave attenuation in the central and Eastern Alborz. *Seismol. Soc. Am., Bull.*, **105**(3), doi: 10.1785/012014049.

25. AllamehZadeh, M., Farahbod, A.M., Hatzfeld, D., Mokhtari, M., Moradi, A.S., Mostafazadeh, M., Paul, A., and Tatar, M. (2004) Seismological aspects of 26 December 2003 Bam earthquake and its aftershock analysis. *Earthquake Spectra*, Special Issue.

26. Vazirzade, S.M., Nozhati, S., and AllamehZadeh, M. (In Press) Seismic reliability assessment of structures using artificial neural network. *Journal of Building Engineering*, http://doi.org/10.1016/j.jobe.2017.04.001.